DEPENDENCE BETWEEN THE SIZE OF THE TREATMENT ROOM AND THE FLUENCE OF NEUTRONS UNDESIRABLE IN RADIOTHERAPY FOR THE HIGH-ENERGY THERAPEUTIC X-RAYS GENERATED BY THE LINEAR MEDICAL ACCELERATOR*

Marcin Łaciak, Adam Konefał

Department of Nuclear Physics and Its Application
Institute of Physics University of Silesia
Uniwersytecka 4, 40-007 Katowice, Poland

The medical linear accelerator is a very commonly used therapeutic equipment in modern radiotherapy. The high-energy X-ray beams generated by such accelerators induce neutrons undesirable in the radiotherapy treatment. The neutron radiation is produced mainly in (γ,n) and $(\gamma,2n)$ reactions. The problem of induced neutron radiation during emission of high-energy X-ray beams is known but it is still unsolved. The undesirable neutrons induce radioactivity inside the treatment room as well as they are the factor of the additional total body dose to patients. The induced radioactivity gives its contribution to the dose to staff operating an accelerator. The influence of sizes of the treatment room on the neutron fluence in the vicinity of the accelerator was investigated in the presented studies. Two methods were applied. The main one was the Monte Carlo computer simulations based on the Geant4 code. These Monte Carlo calculations were verified by means of the neutron activation method with the use of the indium foil and cadmium in the range of thermal and resonance energies. The performed studies are indicative that there is a sensitive dependence between the treatment room size and the neutron level. The greater neutron fluence was observed for a less treatment room.

1. Introduction

At present, the medical linear accelerators are the main source of the therapeutic beams used in classical radiotherapy. These accelerators can

---

generate X-ray and electron beams with energies up to even 25 MeV. The high-energy therapeutic beams are contaminated by neutrons induced in photonuclear $(\gamma,n)/(\gamma,2n)$ and electronuclear $(e, e'n)$ reactions [1–3]. The produced neutrons are characterized by a broad energy spectrum from thermal energy up to even 10 MeV or more [4, 5]. The problem of the neutron contamination is particularly significant for the X-ray beams because cross sections of photonuclear reactions are about two orders of magnitude greater than those for electronuclear reactions in the range of energies used in radiotherapy [6]. The dependence between the neutron fluence in the treatment room and various factors was investigated in many works. It turn out that the neutron fluence depends strongly on the kind and energy of the treatment beam [7–10] as well as on a construction of the accelerator [11]. The level of neutrons produced by X-ray beams is over one order of magnitude greater than that for electron beams [7, 8]. The main sources of neutrons are components of the medical accelerator head made of materials with high-Z, *i.e.* a target, a flatting filter and collimators made of heavy metals [12]. The neutrons are emitted in all directions and they cause the radioactivity of objects in the treatment room [13, 14]. This radioactivity is induced mainly in simple capture reactions (n,γ) occurring for all isotopes. These reactions are characterized by relatively large cross sections at thermal and resonance energies of neutrons. The radioactivity induced in the treatment room increases the radiation doses to staff operating accelerators. Moreover, patients are given the additional total body dose from fast neutron mainly. In the literature, there is a lack of an effective procedure saying how to reduce the neutron fluence in the treatment rooms. In this paper, the investigations of the influence of the treatment room size on the induced neutron level are presented. The studies were performed for the 20 MV X-ray beam from the medical linac Clinac 2300 by Varian. The main part of the work was carried out with the use of Monte Carlo calculations realized by computer simulations based on the Geant4 code in version of 4.9.3. This code, created in CERN, contains algorithms making it possible to simulate all processes occurring during emission of the high-energy therapeutic X-ray and electron beams.

2. Materials and methods

2.1. Simulations

The main studies presented in this paper were performed by means of Monte Carlo simulations basing on the Geant4 software package. The high-precision model with the base of cross sections G4NDL 3.12 was applied for simulations of the neutron interactions, whereas the G4EMLOW module of Geant4 was used in simulations of photon and electron processes. The sim-

ulations were carried out for the geometry of the medical linear accelerator Clinac 2300 by Varian. The simulated geometry included the components such as a tungsten–copper target, an iron–tantalum flatting filter, tungsten collimators, magnets and a plastic casing of the linac. Moreover, the treatment room made of concrete, with air inside and logical detectors (volumes filled with air) were defined in the simulation program. The cubic treatment rooms with various lengths of walls were considered. The studies were performed for the lengths of the walls of $8 \text{ m} \times 8$ m, $10 \text{ m} \times 10$ m and $14 \text{ m} \times 14$ m. The height of the treatment room (the distance from the surface of the floor to the one of the ceiling) was 3 m, whereas the thickness of the walls was 1.5 m (typical for treatment rooms with medical linear accelerators). The simulations started from the electron beam hitting the target. Energy of the electron beam before the target (according to the recommendations by the manufacturer) was 22.3 MeV. The visualisation of the chosen fragments of the simulated system and the scheme of the simulated treatment room with indicated logical detectors are presented in figure 1. The detectors B, C and D were placed on the walls symmetrically in relation to the accelerator head. The detector A was located under the accelerator head.
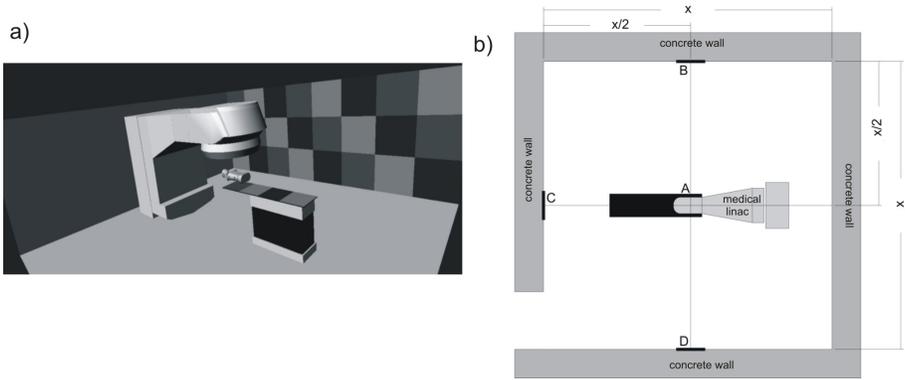

Fig. 1. (a) The visualisation of the fragment of the simulated system (the accelerator, treatment couch, an humanoid phantom, and the fragment of walls and floor). (b) The scheme of the simulated treatment room with the logical detectors registered energies of neutrons. In the presented simulations, the length of the wall x was equal to 8 m, 10 m and 14 m.

2.2. Measurements

The simulation program was verified by measurements of the neutron fluence in the range of thermal and resonance energies. The measurements were carried out with the use of the neutron activation method. The indium foils (^{115}In isotope) were applied as neutron activation detectors. The foil density was 100–110 mg/cm^2. Isotope ^{115}In has a relatively high cross

section for thermal neutron simple capture reaction (160 barns [15]). It also exhibits a high resonance peak at 1.45 eV (about 28 000 barns [16]) and a number of lower resonances in the resonance energy range, yielding the resonance activation integral of 2700 barns [17]. The thermal and resonance neutrons induce the activity of the foil in the reaction: ^{115}In $+$ n, giving the metastable state ^{116m}In ($T_{1/2} = 54.41$ min.) followed by the radioactive β_- decay giving the state ^{116}Sn*. There is a dependence between the foil activity induced by neutrons and the thermal/resonance neutron fluence. In the presented investigations, the activities of the indium foils were determined on the base of measurements of the gamma energy spectrum from the deexcitation of the state ^{116}Sn*. The spectral measurements were performed using a Ge(Li) detector. The activities of the foils were determined by counting the photons of 1293.54 keV. The Ge(Li) detector was calibrated with the use of the 1332.50 keV photons from a ^{60}Co source with the same shape and surface as the used indium foils. The cadmium cover method was applied to separate the foil activity due to thermal and resonance neutrons. The total activity in the indium foil covered by cadmium is induced by resonance neutrons. However, the difference between the activity induced in the uncovered foil and the one induced in the foil inside the cadmium shield provides information about the thermal neutrons.

3. Results and discussion

The experimental verification of the simulations was performed with the use of the therapeutic 20 MV X-ray beam from the medical accelerator Clinac 2300 installed inside the typical treatment room in the Centre of Oncology in Gliwice (Poland). The values of neutron fluence measured for this verification were normalized to 1 Gy of the therapeutic maximum X-ray dose in a water phantom, determined according to the recommendations of dosimetry protocols. Such normalization makes it possible to compare the measured neutron fluences with those from the simulations. The final results of the performed verification are presented in Table I. The calculated neutron fluence values turned out to be with a good agreement with the measured ones. The observed differences are within the experimental uncertainty of 30%.

The comparison of calculated neutron fluence values for the different sizes of the treatment room is presented in Table II. The obtained results are divided into three parts. The first column shows the thermal neutron fluence. The second column presents the results for the resonance neutron. In the last column, the neutron fluences for full energy range are included.

The greater neutron fluence was observed for a smaller treatment room. However, the clear dependence between the mean neutron energy registered in the logical detectors and the size of the treatment room did not appear.

TABLE I

The comparison between the neutron fluences derived from the simulations and the measured ones in the range of thermal and resonance neutron energies.

Neutron fluence $\times 10^6$ per 1 Gy of therapeutic maximum X-ray dose [cm^{-2}]				
Logical detector	Thermal energy		Resonance energy	
	Calculated	Measured	Calculated	Measured
detector A	1.8	1.4	1.4	0.9
detector B	1.9	1.7	1.0	1.2
detector C	1.4	1.1	0.7	0.8
detector D	1.8	1.8	0.9	1.2

TABLE II

Neutron fluence for three different sizes of the considered treatment room construction.

Neutron fluence $\times 10^{-3}$ per 10^6 electrons hitting the target [cm^{-2}]			
Length of the walls	Thermal	Resonance	Full spectrum
detector A			
8 m	7.8	3.2	13.9
10 m	6.9	3.0	11.0
14 m	4.1	2.9	8.6
detector B			
8 m	4.4	1.4	8.7
10 m	3.2	1.0	6.2
14 m	2.1	0.6	3.5
detector C			
8 m	3.8	1.0	6.2
10 m	2.6	0.7	4.0
14 m	1.5	0.4	2.3
detector D			
8 m	4.6	1.5	9.2
10 m	3.3	1.1	6.5
14 m	2.2	0.7	3.2

The lowest energy of about 120 keV was registered in the detector C, whereas it was in the range from 310 keV to 330 keV in the detectors B and D. The greatest energy of 395 keV–470 keV was registered in the detector A located under the accelerator. The neutron fluence as well as the neutron energy registered in the logical detectors are strongly affected by physical processes occurring in the concrete. In this medium, the neutrons undergo elastic col-

lisions with nuclei of hydrogen mainly. The slowed down neutrons may get out of concrete and return to air, contributing to the specific distribution of neutron energy in the treatment room. However, there is a lower neutron density inside the larger treatment room. Therefore, the lower neutron fluence appear in the large treatment room.

4. Conclusions

The performed studies indicate that there is a sensitive dependence between the treatment room size and the fluence of neutrons induced by therapeutic high-energy X-rays. The drop in the neutron fluence occurs for the increasing length of the walls of the treatment room in all considered logical detectors. The decrease of the neutron fluence per 1 m of the wall is about 0.5×10^{-3} and 0.1×10^{-3} cm^{-2} per 10^6 electrons hitting the target for thermal and resonance neutrons, respectively for the considered construction of the treatment room. This decrease is approximately 0.9×10^{-3} cm^{-2} per 10^6 primary electrons for the total neutron energy range.

REFERENCES

[1] V. Evdokimoff *et al.*, *Health Phys. Suppl.* **83**, S68 (2002).
[2] A. Konefał *et al.*, *Radiat. Prot. Dosim.* **128**, 133 (2008).
[3] K. Polaczek-Grelik *et al.*, *Appl. Radiat. Isot.* **70**, 2332 (2012).
[4] K. Amgarou *et al.*, *Nucl. Instrum. Methods* **A629**, 329 (2011).
[5] H.R. Vega-Carrillo *et al.*, *J. Radioanal. Nucl. Chem.* **287**, 323 (2011).
[6] D. Ridikas *et al.*, *Nucl. Instrum. Methods* **A562**, 710 (2006).
[7] A. Konefał *et al.*, *Nukleonika* **50**, 73 (2005).
[8] A. Konefał *et al.*, *Physica Medica* **24**, 212 (2008).
[9] C.C. Chen *et al.*, *Nucl. Instrum. Methods* **A562**, 1033 (2006).
[10] A. Naseri, A. Mesbahi, *Rep. Pract. Oncol. Radiother.* **15**, 138 (2010).
[11] J. Gudowska, A. Brahme, *Nukleonika* **41**, 105 (1996).
[12] X.S. Mao *et al.*, *Health Phys.* **72**, 524 (1997).
[13] Wen-Shan Liu *et al.*, *Rad. Phys. Chem.* **80**, 917 (2011).
[14] A. Konefał *et al.*, *Rep. Pract. Oncol. Radiother.* **17**, 339 (2012).
[15] K. Beckurc, K. Wirtc, Niejtronnaja Fizika, Moscow: Atomizdat (1968).
[16] W.J. Price, *Nuclear Radiation Detection*, McGraw-Hill Book Company, USA, 1964.
[17] R.L. Macklin, H.S. Pomerance, *Resonance Capture Integrals*, in: Proceedings of the First International Conference in Peaceful Uses of Atomic Energy, Vol. 5, New York, United Nations, 1956, p. 96.